ACS OMEGA

http://pubs.acs.org/journal/acsodf

Article

# Superamphiphilic Chitosan Cryogels for Continuous Flow Separation of Oil-In-Water Emulsions

Chunpo Gao,[⊥] Yanan Wang,[⊥] Jiasheng Shi, Yanyan Wang, Xiaoli Huang, Xilu Chen, Zhiyong Chen,* Yunfeng Xie,* and Yanzhao Yang*

Cite This: *ACS Omega* 2022, 7, 5937−5945

Read Online

ACCESS | Metrics & More | Article Recommendations | Supporting Information

**ABSTRACT:** Chitosan is a typical hydrophilic biomass building block widely used in material science and engineering. However, its intrinsic amphiphilicity has been seldom noted so far. Herein, a series of glutaraldehyde-crosslinked chitosan cryogels with superamphiphilicity are fabricated at moderately frozen conditions through a freezing−thawing process. The micron-sized porous cryogel samples display a 0° contact angle toward both water and oil, 0° water contact angle under oil, and over 120° oil contact angle underwater. By comparing the wetting behavior of the tablet compressed by pure chitosan powders, the superamphiphilicity of the chitosan sample is proven to be independent on crosslinkers. This special wettability endows the chitosan cryogels with high separation efficiency for various surfactant-stabilized oil-in-water emulsions under continuous flow mode driven by gravity as well as a peristaltic pump.

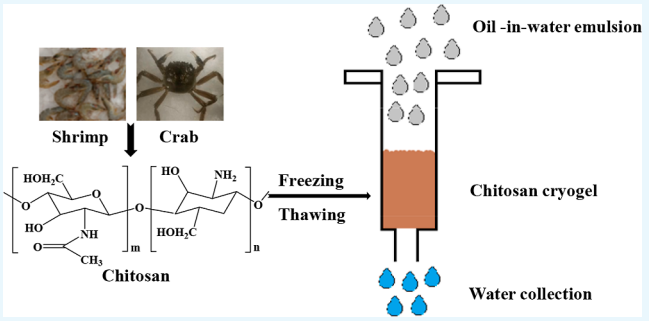


## 1. INTRODUCTION

Chitosan, poly-β-(1,4)-2-amino-2-deoxy-D-glucopyranose, is partially deacetylated from chitin that is the second largest natural materials after cellulose.[1] It is deemed a unique type of cationic carbohydrate based on biomass in the world so far.[2] With an increasing demand on sustainable development, chitosan has been received growing attention and thus has been applied in numerous fields as diverse as drug delivery,[3,4] wound healing,[5] separation media,[6,7] tissue scaffold,[8] and so forth.

One most important feature of chitosan-based materials is porosity that governs mass transfer and site accessibility.[9−12] A variety of porogenic strategies have been developed to construct porous chitosan materials, including ice-template,[13,14] solvent and particle leaching,[15,16] linear polymer removing,[17] and gas forming.[18,19] Among them, the ice-template approach is promising because it fulfills the requirement of green and sustainable development. By virtue of the ice-template approach, supermacroporous chitosan-based materials can be fabricated. Regarding the removal method of ice crystals, the ice-template approach is further classified into two groups, that is, freezing−drying and freezing−thawing. The porous chitosan materials obtained by the freezing−drying process are conventionally termed "aerogel", while those prepared by the freezing−thawing process are usually called "cryogel", though the two definitions are ambiguous and contradictive sometimes in literature.[20,21] Compared to freezing−drying, freezing−thawing could be a better alternative with respect to economic concerns.

Chitosan-based cryogels are designed to gelate under moderately frozen conditions, thus having micron-sized porous structures after ice crystals are removed by the thawing process when the temperature recovers to room temperature.[22] The first report on chitosan-based cryogels was described by Lozinsky and co-workers who found that glutaraldehyde-crosslinked chitosan cryogels showed superior mechanical strength to the samples prepared with the same procedure at the temperature above 0 °C.[23] Nikonorov et al. further studied the detailed conditions, such as temperature, crosslinker content, and molecular weight of chitosan, and how they affect the morphology, gel fraction yield, and swelling property of the samples.[24,25] Zhang et al. systematically investigated the effect of the temperature profile on porous structures of the chitosan-glutaraldehyde systems.[26] Bratskaya et al. proved that diglycidyl ethers can be used as the crosslinker to fabricate chitosan-based cryogels when hydrochloric acid was added in the aqueous system.[27] Besides the pristine chitosan cryogels, numerous composite chitosan-based cryogels have also been

Received: November 3, 2021
Accepted: January 31, 2022
Published: February 11, 2022





https://doi.org/10.1021/acsomega.1c06178
*ACS Omega* 2022, 7, 5937−5945

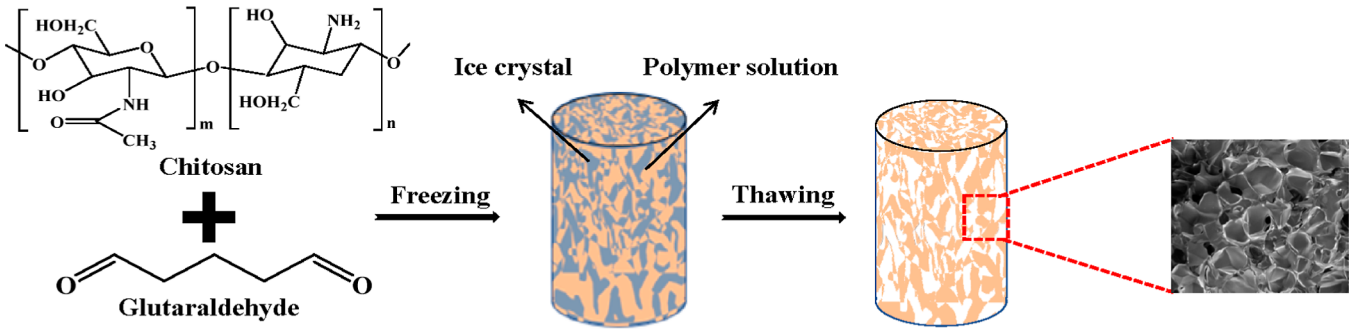


**Figure 1.** Schematic image of fabrication of chitosan-based cryogels by the freezing−thawing process.

developed by cooperating chitosan with cellulose,[28] gelatin,[8] poly(vinyl alcohol),[29] polydopmain,[30] polyurethane,[31] and so on.

Water pollution has been a challenging issue in recent years due to an increasing oil spill accidents and industrial destroy incidents.[32,33] Oil/water separation, especially oil-in-water emulsion separation, has attracted a growing attention around the world.[34,35] Due to their supermacroporosity of cryogels, several types of cryogels, including rubber-graphite-based[36] and polymethacrylate-based cryogels,[37−39] have successfully been applied in rapid separation of the oil/water mixture. In our previous study, the composite cryogels based on polyethylene glycol incorporated with hydrophobic polydivinyl benzene particles displayed high separation efficiency for the surfactant-stabilized oil-in-water emulsions.[40] Nevertheless, the cryogels involved in oil/water separation are limited up to now, and such functional cryogels above are derived from fossil-based raw materials. Thus, it is very desirable that biomass-based cryogels are explored in emulsion separation.

In this work, we aim to demonstrate the potential of chitosan cryogels based on the freezing−thawing process in the separation of surfactant-stabilized oil-in-water emulsions. We noted that chitosan is well known as a kind of hydrophilic building block. In order to achieve separation of oil/water mixture or emulsion, several chitosan aerogels are reported to convert their hydrophilic surfaces into hydrophobic ones before treatment of wastewater.[41−43] During our preliminary tests on chitosan-based cryogels, we unexpectedly observed that the near chitosan cryogels displayed superamphiphilic wetting behavior because the samples show 0° contact angle toward both water and oil in air. Based on the literature and our previous experience,[40,44,45] the superamphiphilic foams are of high separation efficacy of oil-in-water emulsion. These considerations stimulated us to investigate the possibility of the pristine chitosan cryogels in separation of oil-in-water emulsion. Three types of oil-in-water emulsions, stabilized by cationic, nonionic, and anionic surfactants, respectively, were chosen to verify the universality of our method. The chitosan cryogels were tested to show rapid separation of various oil-in-water emulsions under continuous flow mode driven by gravity as well as a peristaltic pump.

## 2. RESULTS AND DISCUSSION

**2.1. Supermacroporous Chitosan Cryogels Fabricated by Freezing−Thawing.** Chitosan cryogels were obtained through Schiff base crosslinking reaction between amino groups on chitosan and aldehyde groups on glutaraldehyde during a freezing−thawing process (Figure 1). In the moderately frozen condition, water molecules converted into ice crystals; due to the cryoconcentration effect,[22] the gelation induced by Schiff base reaction could still occur at the sub-zero temperature (−18 °C); when the temperature was increased up to room temperature, ice crystals were thawed, leaving the supermacroporous structures in the original matrix. Such a freezing−thawing process is much greener and more economic than the freezing−drying process.

Results of yield of chitosan−glutaraldehyde cryogels varying with glutaraldehyde content are shown in Table 1. The gel

**Table 1. Yield of Chitosan-Based Cryogels Obtained at 2.0 wt % Chitosan Loading Amount With Glutaraldehyde as the Crosslinker**

| crosslinker content (vol %) | gel yield (%) | | | |
|---|---|---|---|---|
| | 1 | 2 | 3 | average ± standard deviation |
| 0.1 | 77.3 | 75.7 | 79.5 | 77.5 ± 1.6 |
| 0.2 | 80.4 | 77.0 | 80.8 | 79.4 ± 1.7 |
| 0.3 | 76.8 | 75.0 | 75.5 | 75.8 ± 0.7 |
| 0.4 | 80.1 | 83.4 | 79.7 | 81.1 ± 1.6 |
| 0.5 | 76.6 | 74.0 | 81.8 | 77.2 ± 2.9 |

yields achieve around 80% and are independent on glutaraldehyde content at 2.0 vol % chitosan loading amount, indicating high crosslinking efficiency of Schiff base reaction under the conditions. Such Schiff base reaction was confirmed by infrared spectroscopy, as shown in Figure 2. Besides specific peaks of chitosan, a new peak appears at 1665 $cm^{-1}$, which corresponds to the formation of the C=N bond,[19,46] in comparison with the peak at 1653 $cm^{-1}$ assigned to the C−N bond on chitosan.

The supermacroporosity of the chitosan-based cryogels was observed by scanning electron microscopy (Figure 3). The samples display micron-sized porous structures and similar morphology under the cross-section view as well as side-section view. The results strongly indicate that the porous structures are interconnected in the matrix and probably suitable for rapid mass transfer in real application. Additionally, no significant difference could be found in the porous structures between the two samples obtained at 0.2 and 0.5% crosslinker content according to SEM images, implying that supermacroporous structures could be mainly attributed to the amount and shape of ice crystals. Thermal gravity analysis shows a two-step weight loss for the samples (Figure S1). The decrease in weight at below 100 °C is possibly attributed to bound water loss, and the corresponding loss at over 220 °C should result from degradation of the chitosan backbone. Half-



https://doi.org/10.1021/acsomega.1c06178
ACS Omega 2022, 7, 5937−5945

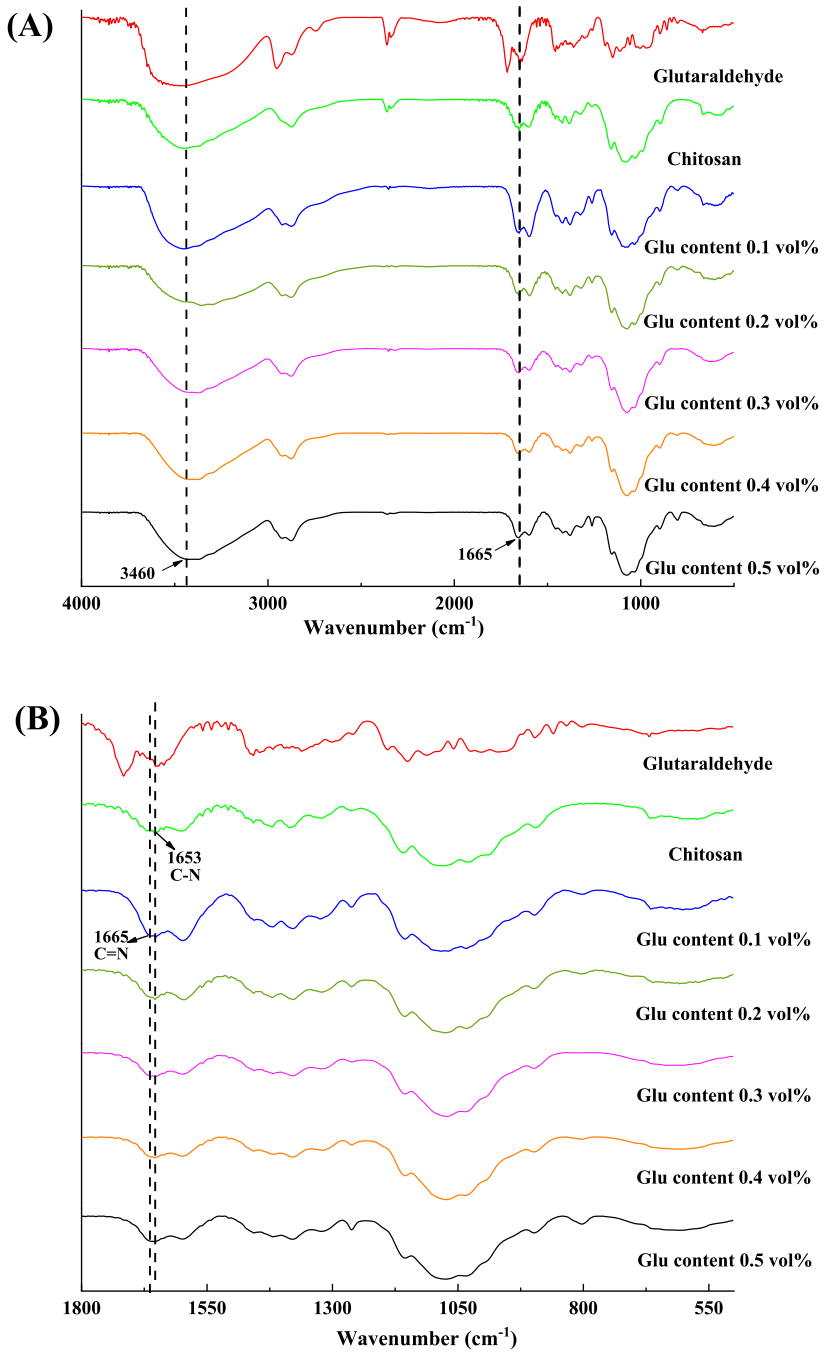


**Figure 2.** FTIR spectra of chitosan cryogels prepared by different crosslinker contents with full scale (A) and magnification from 500 to 1800 $cm^{-1}$ (B).

life temperatures of the samples with glu content 0.2 and 0.5% are 282 and 293 °C, respectively.

The supermacroporosity of the chitosan-based cryogels was further investigated by the mercury intrusion method. As shown in Figure 4A, the pore sizes of the two chitosan samples mainly lie in the range of 20 to 120 $\mu$m, which are well consistent with the results obtained by SEM. The average pore size of the sample obtained at 0.5% crosslinker is slightly smaller than that obtained at 0.2% crosslinker (Table 2), possibly due to the shrinking of the matrix driven by the greater amount of the Schiff base bond.

In order to further study the mesoporous and microporous structure of the samples, nitrogen adsorption tests were adopted. As shown in Figure 4B, a large hysteresis loop is found in the adsorption−desorption curve ranging from 0.4 to 0.9 relative pressure for the two samples. The results indicate that a number of both mesoporous (2−50 nm) and macroporous (greater than 50 nm) structures exist in the samples, as also shown in pore size distribution curves (Figure 4C). Similar to the results observed by mercury intrusion, the lower crosslinked sample displays a greater average pore size compared to the higher crosslinked one (Table 2). Nevertheless, both of two samples have a very low surface area below 5.0 $m^2/g$, which is a characteristic feature for most cryogel materials.[22,50]



https://doi.org/10.1021/acsomega.1c06178
ACS Omega 2022, 7, 5937−5945

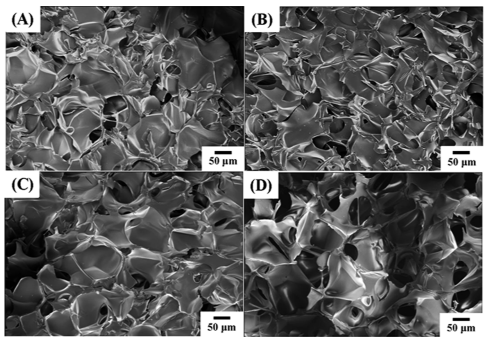


**Figure 3.** SEM images of chitosan cryogels prepared by different conditions. (A) Cross-section view, glutaraldehyde content, 0.2 vol %, (B) side-section view, glutaraldehyde content, 0.2 vol %, (C) cross-section view, glutaraldehyde content, 0.5 vol %, and (D) side-section view, glutaraldehyde content, 0.5 vol %.

**2.2. Superamphiphilicity of Chitosan Cryogels.** Wettability is deemed a crucially important factor in separation of oil-in-water emulsion.[42,43] Figure 5 shows contact angle tests for chitosan−glutaraldehyde cryogel samples under different conditions. Chitosan is regarded as a typical hydrophilic material; however, in our cases, it is observed that the chitosan−glutaraldehyde cryogel samples display superphilicity both to water and to oil in air as water contact angle (WCA) as well as oil contact angle (OCA) both are 0°. Moreover, they have 0° WCA under oil but over 120° OCA underwater (Table 3). Among them, the sample with 0.2% glu content shows 141.5° ± 1.3° of OCA underwater, and the sample with 0.5% glu content has 128.6° ± 2.5° of OCA underwater. This unique wettability probably gives a great potential for the material in oil-in-water emulsion separation.

To further investigate the origination of the special wettability of the chitosan-based cryogels, we compared the difference between the pure chitosan and chitosan−glutaraldehyde cryogel sample in dye diffusion. Given that pure chitosan cannot form the gel sample under the used condition, chitosan powders were compressed into a thin round slice (12.6 mm in diameter and 0.3 mm in thickness) as control. As shown in Figure 6A and Movie S1, both water and oil droplets can spread the surface of the chitosan−glutaraldehyde cryogel sample, which is similar to that observed on the pure chitosan slice (Figure 6B, Movie S2). The results strongly indicate that the superamphiphilicity of the chitosan sample is an intrinsic property of chitosan, which is independent of the involvement of glutaraldehyde. As well known, chitosan is a typical hydrophilic material, and the amphiphilicity of pure chitosan

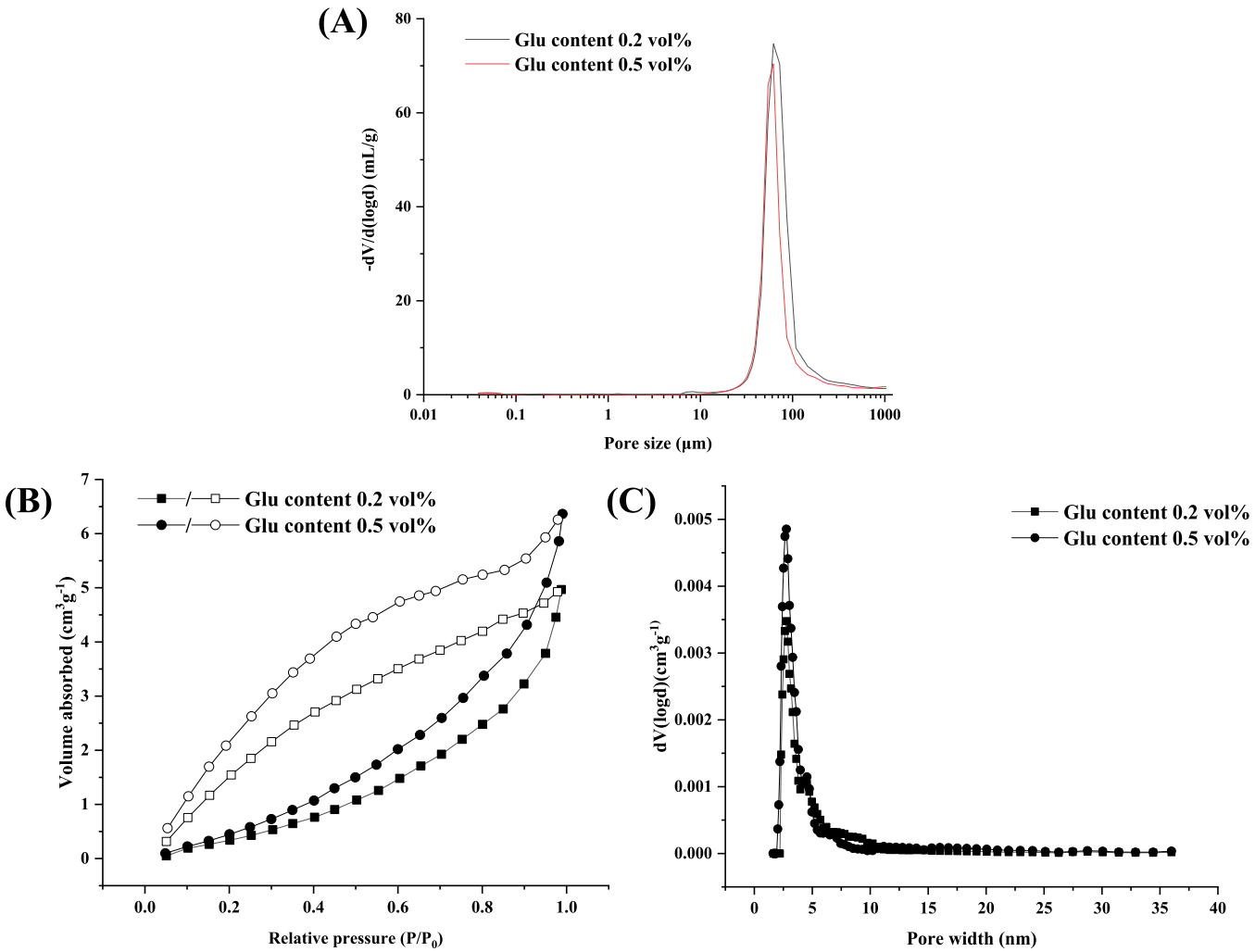


**Figure 4.** Pore-size distribution of chitosan cryogels prepared with different procedures based on mercury intrusion porosimetry (A). Nitrogen adsorption (closed)/desorption (open) isotherms of samples at 77.3 K (B) and pore size distribution curves calculated using the DFT method (C).



https://doi.org/10.1021/acsomega.1c06178
ACS Omega 2022, 7, 5937−5945

Table 2. Pore Characteristic Features of Different Samples

| crosslinker content (vol %) | nitrogen adsorption | | | mercury intrusion porosimetry | | |
|---|---|---|---|---|---|---|
| | $S_{BET}$[a] ($m^2\ g^{-1}$) | $PV_{BET}$[b] ($cm^3\ g^{-1}$) | average pore diameter (nm) | total surface area ($m^2\ g^{-1}$) | $PV_{MIP}$[c] ($cm^3\ g^{-1}$) | average pore diameter ($\mu$m) |
| 0.2 | 3.5 | $0.7*10^{-3}$ | 12.5 | 11.2 | 23.8 | 80.8 |
| 0.5 | 4.8 | $0.9*10^{-3}$ | 7.0 | 8.8 | 19.1 | 78.2 |

[a]Surface area calculated from the nitrogen adsorption isotherms at 77.3 K using the BET method. [b]Pore volume calculated from the nitrogen adsorption isotherms at $P/P_0$ = 0.99, 77.3 K. [c]Pore volume calculated from mercury intrusion porosimetry.

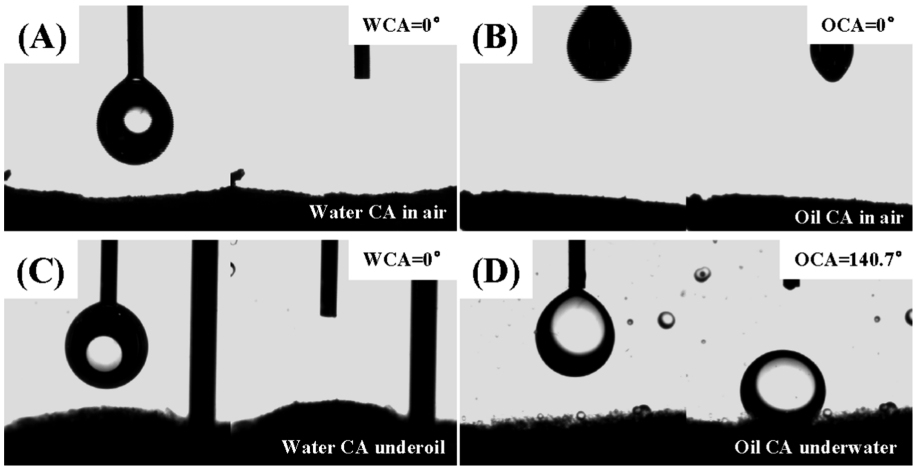


Figure 5. Water contact angle (WCA) in air (A), oil contact angle (OCA, toluene) in air (B), WCA underoil (C), and oil (DCE) CA (OCA, D) underwater of the chitosan−glutaraldehyde cryogel (glu, 0.2 vol %) sample with 3.0 $\mu$L droplet volume.

Table 3. Contact Angles of Different Chitosan Cryogels[a]

| crosslinker content (vol %) | test condition | 1 (°) | 2 (°) | 3 (°) | average ±standard deviation (°) |
|---|---|---|---|---|---|
| 0.2 | WCA in air | 0 | 0 | 0 | 0 ± 0 |
| | OCA in air | 0 | 0 | 0 | 0 ± 0 |
| | WCA underoil | 0 | 0 | 0 | 0 ± 0 |
| | OCA underwater | 140.4 | 143.3 | 140.7 | 141.5 ± 1.3 |
| 0.5 | WCA in air | 0 | 0 | 0 | 0 ± 0 |
| | OCA in air | 0 | 0 | 0 | 0 ± 0 |
| | WCA underoil | 0 | 0 | 0 | 0 ± 0 |
| | OCA underwater | 126.2 | 127.4 | 132.1 | 128.6 ± 2.5 |

[a]Note: droplet volume 3.0 $\mu$L.

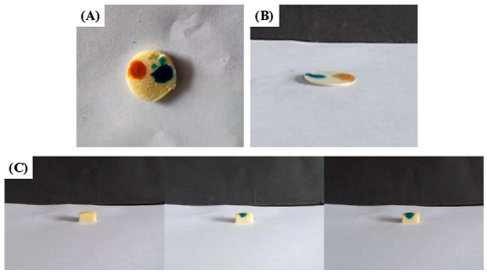


Figure 6. Optical images of droplets of methylene blue stained water and methyl red stained oil spreading on the surface of the chitosan−glutaraldehyde cryogel (glu, 0.2 vol %) sample (A) and the tablet compressed by pure chitosan powders (B). Diffusion of methylene blue stained water through the chitosan−glutaraldehyde cryogel (glu, 0.2 vol %) sample (C).

has seldom been reported so far to our knowledge. The actual explanation for such superamphiphilicity is not clear at present; however, we deduce that pure chitosan must possess two regions, that is, hydrophilic region and hydrophobic region, and the latter may be possibly attributed to the strong intramolecular hydrogen bondings derived by the interaction among amino groups and hydroxyl groups. When observed from the side view, the water solution dyed by methylene blue can rapidly pass through the chitosan−glutaraldehyde column sample in a valley shape under gravity (Figure 6C, Movie S3), confirming that the porous structures of the sample are interconnected, as seen in SEM images.

**2.3. Separation of Oil-In-Water Emulsions.** The unique wettability and the convective porous structures of the chitosan−glutaraldehyde cryogels prompted us to use it in the field of oil-in-water emulsion separation. Three types of surfactant-stabilized oil-in-water emulsions were chosen to test separation performance under continuous flow mode. Before treatment of emulsion, the dried cryogel sample rapidly adsorbed water to achieve equilibrium within 2 h (Figure S2). As shown in Figure 7, after the milky emulsion is added into the syringe, a clear and transparent solution can be collected at the bottom of the syringe under gravity. Micron-sized surfactant-stabilized oil droplets can hardly be seen after treating the emulsion by the chitosan sample. The subsequent


https://doi.org/10.1021/acsomega.1c06178
ACS Omega 2022, 7, 5937−5945

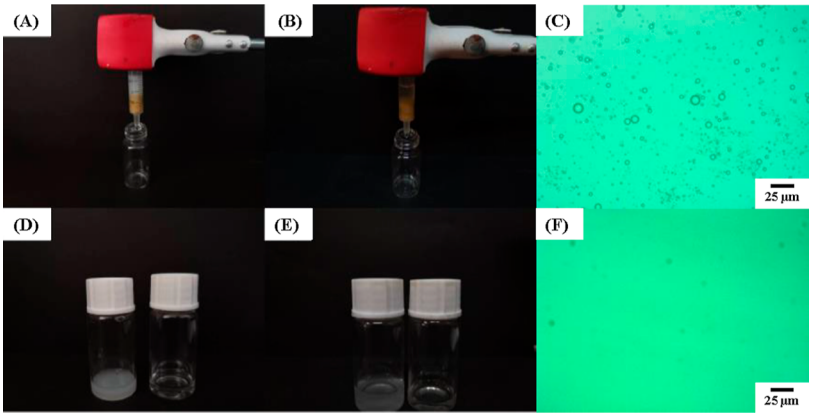


**Figure 7.** Separation performance of the chitosan−glutaraldehyde cryogel (glu, 0.2 vol %) sample toward Tween-80 stabilized toluene-in-water emulsion (A,D) and SLS stabilized toluene-in-water emulsion (B,E), respectively. Optical images of separation of Tween-80 stabilized toluene-in-water emulsion before (C) and after (F) using the chitosan cryogel, respectively.

measurements confirmed that the separation efficiency can reach above 96% for three types of emulsions using five chitosan−glutaraldehyde cryogel samples with different crosslinker contents, respectively (Table 4). The results indicated that three processes, including demulsification, adsorption, and separation, can be integrated into one-step process conducted on the chitosan-based columns, showing a very promising possibility for rapid separation of various oil-in-water emulsions.

**Table 4. Separation Efficiency of Emulsions by Chitosan Cryogels Under Gravity**

| | separation efficiency (%) | | | |
|---|---|---|---|---|
| crosslinker content (vol %) | sodium lauryl sulfate | Tween-80 | cetyl trimethyl bromide | average ±standard deviation |
| 0.1 | 98.0 | 97.7 | 98.0 | 97.9 ± 0.1 |
| 0.2 | 97.5 | 98.1 | 96.7 | 97.4 ± 0.6 |
| 0.3 | 97.0 | 97.8 | 97.9 | 97.6 ± 0.4 |
| 0.4 | 98.8 | 97.6 | 97.7 | 98.0 ± 0.5 |
| 0.5 | 95.9 | 97.2 | 95.5 | 96.2 ± 0.7 |

The exact mechanism of emulsion separation has been the subject of considerable controversy.[42,43] In our cases, the unique wetting behavior of chitosan-based cryogels, that is, the superphilicity to water under oil and oleophobicity to oil under water, could be favorable for demulsification. According to infused-liquid switchable behavior described by Wang et al., whether liquid can be infused in the matrix is dependent on the polar part of the surface energy (PSE) of the liquid.[47] As toluene has a lower PSE compared to water, toluene can be repelled by water even if toluene molecules first occupy inside the room of the porous superamphiphilic matrix. As such, water molecules can pass through the chitosan-based column, while toluene molecules are blocked by the oleophobic sample under the aqueous conditions. This behavior is usually found in oil-blocking type separation based on superwetting materials.[44] Tracking the surfactant confirms that only 35.7 ± 7.0% of Tween 80 can be found in the filtrate, indicating that most of the surfactants can be adsorbed by the chitosan-based column. Meanwhile, 97.7 ± 1.8% of water molecules can pass through the chitosan-based column (Table S3). Given that the average pore size of the chitosan cryogel is significantly greater than the particle size of the oil-in water emulsion (Figure 7c, Table S2, and Figure S2), the "size screening" should be not a main driven force for demulsification in our cases.[48,49]

The continuous separation of emulsion by the chitosan-based cryogel sample was further performed on a homemade device driven by a peristaltic pump at a 480 mL/h flow rate.

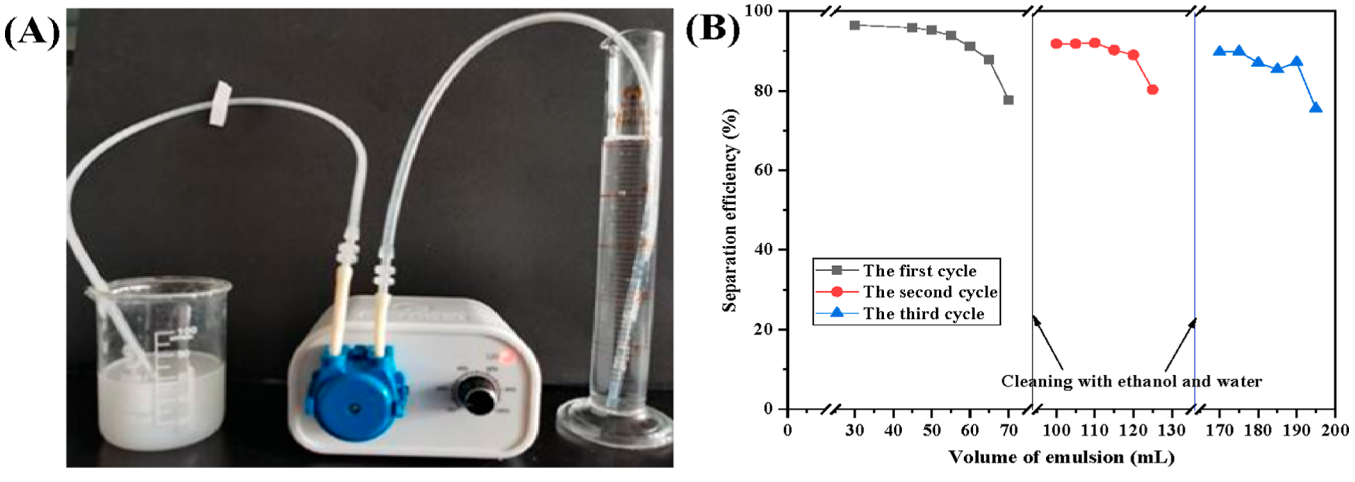


**Figure 8.** Homemade device for continuous separation of emulsion (A). Recyclability of the chitosan cryogel sample (B).



https://doi.org/10.1021/acsomega.1c06178
ACS Omega 2022, 7, 5937−5945

The chitosan-based cryogel is located in the top part of the plastic tube that is immersed in oil-in-water emulsion. With the emulsion pumped in the first tube, clear and transparent solution can be accumulated in the reservoir connected with the second tube (Figure 8A). As the pumped-out volume of the emulsion reaches 50 mL, 25 times volume of the chitosan-based cryogel sample, the separation efficiency is still over 95% and maintains above 77% on further loading emulsion to 70 mL (Figure 8B). Besides, after being washed by ethanol and water, the chitosan-based cryogel column can be recycled for continuous separation of surfactant-stabilized oil-in-water emulsion with high efficiency in the two subsequent treatments.

## 3. CONCLUSIONS

A series of glutaraldehyde crosslinked chitosan cryogels were fabricated at moderately frozen conditions through a freezing−thawing process. Based on tests by SEM and mercury intrusion, the obtained cryogels were demonstrated to have micron-sized porous structures that are interconnected and averaged around 80 $\mu$m in pore size. Moreover, nitrogen adsorption tests confirmed that the samples had a small amount of mesoporous and microporous structures. Contact angle studies indicated for the first time that chitosan-based cryogels showed superphilicity both to water and to oil in air, superphilicity to water under oil, as well as oleophobicity to oil underwater. After investigation on the wetting behavior of the tablet composed of pure chitosan powders, the super-amphiphilicity of the chitosan sample was demonstrated to be an intrinsic property of chitosan. The chitosan cryogels with special wettability showed high separation efficiency for various surfactant stabilized oil-in-water emulsions even under high flow speed driven by a pump, showing a promising potential in large-scale treatment of oil-in-water emulsions.

## 4. MATERIALS AND METHODS

**4.1. Materials.** Chitosan (CTS, 98% deacetylation, 100−200 mpa/s) and glutaraldehyde (Glu) were obtained from Aladdin Chemistry Co., Ltd. (Shanghai, China). Acetic acid (AA), ethanol, 1,2-dichloroethane (DCE), and toluene were purchased from Fuyu Chemical Reagent Co., Ltd. (Tianjin, China). Tween-80, sodium lauryl sulfate (SLS), and cetyl trimethyl bromide (CTEB) are all from Sinopharm Chemical Regent Co. Ltd. (Shanghai, China).

**4.2. Fabrication of Chitosan-Based Cryogels.** Chitosan-based cryogels were fabricated at a moderately frozen condition according to the previous studies with slight modifications.[22−25] Typically, a chitosan stock solution was first prepared by adding 2 g of chitosan into 100 mL of water containing 2.0 vol % of acetic acid with vigorously stirring at 75 °C for 2 h. Then, 2 mL of the stock chitosan solution was taken out and mixed with 4 $\mu$L of glutaraldehyde (0.2 vol %) into a sealed plastic syringe with a capacity of 5 mL. The sealed syringe was placed in a freezer at −18 °C for 24 h and then thawed at room temperature. After that, the resulting material was successively washed by NaOH aqueous solution (1.0 wt %), water, and ethanol and finally dried at 50 °C to constant weight.

**4.3. Characterization.** Fourier-transform infrared spectroscopy (FTIR, Spectrum one, PerkinElmer, Waltham, MA) was used to characterize the occurrence of the reaction. Scanning electron microscopy (SEM, FEI QUANTA FEG250) was used to investigate the pore structure of the samples. Both nitrogen adsorption (ASAP 2020 M, Micromeritics, Norcross, GA) and mercury intrusion porosimetry (Poremastier-60, Quantachrome, Boynton Beach, FL) tests were used to measure the pore size and its distribution of the resultant material.[50] The wettability of the sample was studied by measuring the contact angle (CA) on an instrument (OCA 40, Dataphysics, Germany) at room temperature. Also, the CA was measured in several environments including in air, underwater, and under oil. The thermal stability of the samples was measured by Diamond TG/DTA (PerkinElmer, Shanghai, China) by heating each sample from 25 to 800 °C, with a heating rate 10 °C/min under a nitrogen atmosphere. The size distribution of emulsion was further measured by a dynamic light scattering nanosizer (DLS, Nano-ZS 3600, Malvern, UK) at room temperature.

**4.4. Separation of Oil-In-Water Emulsions.** Three types of oil-in-water emulsions were prepared according to previous studies.[40] Toluene (495 $\mu$L), 50 mg of surfactant (Tween-80, sodium lauryl sulfate or cetyl trimethyl bromide), and 45 mL of deionized water were mixed by stirring for 24 h. The volume ratio of oil to water was 1:100. The obtained emulsions were stable at least within 1 week.

The cryogel sample was put into a plastic syringe and swollen in water for 2 h to achieve equilibrium before separation. The oil-in-water emulsion (1 mL) was added to the syringe and passed through the sample under gravity. The remnant toluene in water was extracted by 3.0 mL of carbon tetrachloride, and its content was measured at 265 nm by an ultraviolet−visible-light (UV−vis) spectrometer (UV759CRT, Yoke Instrument Co. Ltd., Shanghai, China). The separation efficiency (SE) could be calculated by the equation as follows

$$\mathrm{SE} = (1 - C_f/C_0) \times 100\%$$

where $C_0$ and $C_f$ are the concentration of toluene in water before and after separation, respectively. After the separation, the samples were washed with ethanol for recycling. Separation of oil-in-water emulsions under another continuous flow mode was conducted using a peristaltic pump.[51] Before and after separation, oil-in-water emulsions were also observed by an optical microscope (Nikon Eclipse LV100 POL).

**4.5. Swelling Ratios of Cryogels.** The dried samples with 1 cm length were accurately weighted ($W_d$). Then, the samples were put into 10 mL of water and taken out every 20 min from water at room temperature. After removal of the surface water of the cryogel sample by the weight papers, the samples were then weighted ($W_s$). The swelling ratio of the sample was calculated by the following equation

$$\text{swelling ratio} = (W_s - W_d)/W_d$$

**4.6. Determination of Tween 80 in Filtrate.** The concentration of Tween 80 in the filtrate was determined based on a quantitative test for the complex of the polyoxyethylene groups of Tween with $NH_4[Co(SCN)_3]$ according to literature.[40,52] The absorption of the complex solution was measured at 624 nm using an UV−vis spectrometer (UV759CRT, Yoke Instrument Co. Ltd., Shanghai, China).

## ■ ASSOCIATED CONTENT

### Supporting Information

The Supporting Information is available free of charge at https://pubs.acs.org/doi/10.1021/acsomega.1c06178.



https://doi.org/10.1021/acsomega.1c06178
ACS Omega 2022, 7, 5937−5945

TGA curves and swelling ratios of the samples, concentration of Tween 80 in the filtrate, and size distribution of Tween-80-stabilized toluene-in-water emulsion measured by DLS (PDF)

Spreading processes of water and oil droplets on the chitosan cryogel slice samples (AVI)

Spreading processes of water and oil droplets on the pure chitosan sample (AVI)

Diffusion process of methylene blue-stained water through the samples (AVI)

## AUTHOR INFORMATION


### Corresponding Authors

**Zhiyong Chen** − *Shandong Provincial Key Laboratory of Fluorine Chemistry and Chemical Materials, School of Chemistry and Chemical Engineering, University of Jinan, Jinan 250022, People's Republic of China;* orcid.org/0000-0003-2309-775X; Email: chm_chenzy@ujn.edu.cn

**Yunfeng Xie** − *Beijing Key Laboratory of Nutrition & Health and Food Safety, Nutrition & Health Research Institute, COFCO Corporation, Beijing 102209, People's Republic of China*; Email: xieyunfeng@cofco.com

**Yanzhao Yang** − *School of Chemistry and Chemical Engineering, Shandong University, Jinan 250100, People's Republic of China;* orcid.org/0000-0001-7443-8417; Email: yzhyang@sdu.edu.cn

### Authors

**Chunpo Gao** − *School of Chemistry and Chemical Engineering, Shandong University, Jinan 250100, People's Republic of China; Shandong Hongjitang Pharmaceutical Group CO. Ltd, Jinan 250103, People's Republic of China*

**Yanan Wang** − *Shandong Provincial Key Laboratory of Fluorine Chemistry and Chemical Materials, School of Chemistry and Chemical Engineering, University of Jinan, Jinan 250022, People's Republic of China*

**Jiasheng Shi** − *Shandong Provincial Key Laboratory of Fluorine Chemistry and Chemical Materials, School of Chemistry and Chemical Engineering, University of Jinan, Jinan 250022, People's Republic of China*

**Yanyan Wang** − *Shandong Provincial Key Laboratory of Fluorine Chemistry and Chemical Materials, School of Chemistry and Chemical Engineering, University of Jinan, Jinan 250022, People's Republic of China*

**Xiaoli Huang** − *Shandong Provincial Key Laboratory of Fluorine Chemistry and Chemical Materials, School of Chemistry and Chemical Engineering, University of Jinan, Jinan 250022, People's Republic of China*

**Xilu Chen** − *Shandong Hongjitang Pharmaceutical Group CO. Ltd, Jinan 250103, People's Republic of China*

Complete contact information is available at: https://pubs.acs.org/10.1021/acsomega.1c06178

### Author Contributions

⊥C.G. and W.Y.contributed to this work

### Notes

The authors declare no competing financial interest.


## ACKNOWLEDGMENTS

The authors gratefully thank National Key R&D Program of China (no. 2017YFC1600404) and National Natural Science Foundation of China (no. 22178199 and 51873079) for financial support. The research was also financially supported by Open Projects Fund of Shandong Key Laboratory of Carbohydrate Chemistry and Glycobiology, Shandong University (no. 2019CCG02) and Science and Technology Bureau of Jinan City (2021GXRC105).

## REFERENCES


(1) Khan, A.; Alamry, K. A. Recent Advances of Emerging Green Chitosan-Based Biomaterials with Potential Biomedical Applications: A Review. *Carbohydr. Res.* **2021**, *506*, 108368.

(2) Sadiq, A. C.; Olasupo, A.; Ngah, W. S. W.; Rahim, N. Y.; Suah, F. B. M. A Decade Development in The Application of Chitosan-Based Materials for Dye Adsorption: A Short Review. *Int. J. Biol. Macromol.* **2021**, *191*, 1151−1163.

(3) Dinu, M. V.; Cocarta, A. I.; Dragan, E. S. Synthesis, Characterization and Drug Release Properties of 3D Chitosan/Clinoptilolite Biocomposite Cryogels. *Carbohydr. Polym.* **2016**, *153*, 203−211.

(4) García-González, C. A.; Sosnik, A.; Kalmár, J.; De Marco, I.; Erkey, C.; Concheiro, A.; Alvarez-Lorenzo, C. Aerogels in Drug Delivery: from Design to Application. *J. Controlled Release* **2021**, *332*, 40−63.

(5) Zhao, X.; Guo, B.; Wu, H.; Liang, Y.; Ma, P. X. Injectable Antibacterial Conductive Nanocomposite Cryogels with Rapid Shape Recovery for Noncompressible Hemorrhage and Wound Healing. *Nat. Commun.* **2018**, *9*, 2784.

(6) Yang, W.-J.; Yuen, A. C. Y.; Li, A.; Lin, B.; Chen, T. B. Y.; Yang, W.; Lu, H.-D.; Yeoh, G. H. Recent Progress in Bio-Based Aerogel Absorbents for Oil/Water Separation. *Cellulose* **2019**, *26*, 6449−6476.

(7) Jaworska, M. M.; Antos, D.; Górak, A. Review on The Application of Chitin and Chitosan in Chromatography. *React. Funct. Polym.* **2020**, *152*, 104606.

(8) Vishnoi, T.; Singh, A.; Teotia, A. K.; Kumar, A. Chitosan-Gelatin-Polypyrrole Cryogel Matrix for Stem Cell Differentiation into Neural Lineage and Sciatic Nerve Regeneration in Peripheral Nerve Injury Model. *ACS Biomater. Sci. Eng.* **2019**, *5*, 3007−3021.

(9) Takeshita, S.; Zhao, S.; Malfait, W. J.; Koebel, M. M. Chemistry of Chitosan Aerogels: Three-Dimensional Pore Control for Tailored Applications. *Angew. Chem. Int. Ed.* **2021**, *60*, 9828−9851.

(10) Dragan, E. S.; Dinu, M. V. Advances in Porous Chitosan-Based Composite Hydrogels: Synthesis and Applications. *React. Funct. Polym.* **2020**, *146*, 104372.

(11) Wei, S.; Ching, Y. C.; Chuah, C. H. Synthesis of Chitosan Aerogels as Promising Carriers for Drug Delivery: A Review. *Carbohydr. Polym.* **2020**, *231*, 115744.

(12) Mohamed, M. G.; Atayde, E. C.; Matsagar, B. M.; Na, J.; Yamauchi, Y.; Wu, K. C.-W.; Kuo, S.-W. Construction Hierarchically Mesoporous/Microporous Materials Based on Block Copolymer and Covalent Organic Framework. *J. Taiwan Inst. Chem. Eng.* **2020**, *112*, 180−192.

(13) Lai, K. C.; Hiew, B. Y. Z.; Lee, L. Y.; Gan, S.; Thangalazhy-Gopakumar, S.; Chiu, W. S.; Khiew, P. S. Ice-Templated Graphene Oxide/Chitosan Aerogel as An Effective Adsorbent for Sequestration of Metanil Yellow Dye. *Bioresour. Technol.* **2019**, *274*, 134−144.

(14) Dinu, M. V.; Přádný, M.; Drăgan, E. S.; Michálek, J. Ice-Templated Hydrogels Based on Chitosan with Tailored Porous Morphology. *Carbohydr. Polym.* **2013**, *94*, 170−178.

(15) Sen, T.; Ozcelik, B.; Ozmen, M. M. Tough and Hierarchical Porous Cryogel Scaffolds Preparation Using n-Butanol as A Non-Solvent. *Int. J. Polym. Mater. Polym. Biomater.* **2018**, *68*, 411−416.

(16) Yang, W.-Y.; Thirumavalavan, M.; Lee, J.-F. Effects of Porogen and Cross-Linking Agents on Improved Properties of Silica-Supported Macroporous Chitosan Membranes for Enzyme Immobilization. *J. Membr. Biol.* **2015**, *248*, 231−240.

(17) Dinu, M. V.; Přádný, M.; Drăgan, E. S.; Michálek, J. Morphogical and Swelling Properties of Porous Hydrogels Based on Poly(Hydroxyethyl Methacrylate) and Chitosan Modulated by Ice-

Templating Process and Porogen Leaching. *J. Polym. Res.* **2013**, *20*, 285.
(18) Kaynak Bayrak, G.; Demirtaş, T. T.; Gümüşderelioğlu, M. Microwave-Induced Biomimetic Approach for Hydroxyapatite Coatings of Chitosan Scaffolds. *Carbohydr. Polym.* **2017**, *157*, 803−813.
(19) Ji, C.; Annabi, N.; Khademhosseini, A.; Dehghani, F. Fabrication of Porous Chitosan Scaffolds for Soft Tissue Engineering Using Dense Gas $CO_2$. *Acta Biomater.* **2011**, *7*, 1653−1664.
(20) Shi, W.; Ching, Y. C.; Chuah, C. H. Preparation of Aerogel Beads and Microspheres Based on Chitosan and Cellulose for Drug Delivery: A Review. *Int. J. Biol. Macromol.* **2021**, *170*, 751−767.
(21) Lozinsky, V. Cryostructuring of Polymeric Systems. 50. Cryogels and Cryotropic Gel-Formation: Terms and Definitions. *Gels* **2018**, *4*, 77.
(22) Lozinsky, V. I. Cryogels on The Basis of Natural and Synthetic Polymers: Preparation, Properties and Applications. *Russ. Chem. Rev.* **2002**, *71*, 489−511.
(23) Lozinsky, V. I.; Vainerman, E. S.; Rogozhin, S. V. Study of Cryostructurization of Polymer Systems. II. The Influence of Freezing of A Reacting Mass on The Properties of Products in The Preparation of Covalently Cross-Linked Gels. *Colloid Polym. Sci.* **1982**, *260*, 776−780.
(24) Nikonorov, V. V.; Ivanov, R. V.; Kil'deeva, N. R.; Bulatnikova, L. N.; Lozinskii, V. I. Synthesis and Characteristics of Cryogels of Chitosan Crosslinked by Glutaric Aldehyde. *Polym. Sci., Ser. A* **2010**, *52*, 828−834.
(25) Nikonorov, V. V.; Ivanov, R. V.; Kil'deeva, N. R.; Lozinskii, V. I. Effect of Polymer Precursor Molecular Mass on The Formation and Properties of Covalently Crosslinked Chitosan Cryogels. *Polym. Sci., Ser. A* **2011**, *53*, 1150−1158.
(26) Zhang, H.; Liu, C.; Chen, L.; Dai, B. Control of Ice Crystal Growth and Its Effect on Porous Structure of Chitosan Cryogels. *Chem. Eng. Sci.* **2019**, *201*, 50−57.
(27) Bratskaya, S.; Privar, Y.; Nesterov, D.; Modin, E.; Kodess, M.; Slobodyuk, A.; Marinin, D.; Pestov, A. Chitosan Gels and Cryogels Cross-Linked with Diglycidyl Ethers of Ethylene Glycol and Polyethylene Glycol in Acidic Media. *Biomacromol* **2019**, *20*, 1635−1643.
(28) Ambaye, T. G.; Vaccari, M.; Prasad, S.; van Hullebusch, E. D.; Rtimi, S. Preparation and Applications of Chitosan and Cellulose Composite Materials. *J. Environ. Manage.* **2022**, *301*, 113850.
(29) Podorozhko, E. A.; Ul'yabaeva, G. R.; Tikhonov, V. E.; Grachev, A. V.; Vladimirov, L. V.; Antonov, Y. A.; Kil'deeva, N. R.; Lozinsky, V. I. A Study of Cryostructuring of Polymer Systems. 43. Characteristics of Microstructure of Chitosan-Containing Complex and Composite Poly(vinyl alcohol) Cryogels. *Colloid J.* **2017**, *79*, 94−105.
(30) Li, M.; Zhang, Z.; Liang, Y.; He, J.; Guo, B. Multifunctional Tissue-Adhesive Cryogel Wound Dressing for Rapid Nonpressing Surface Hemorrhage and Wound Repair. *ACS Appl. Mater. Interfaces* **2020**, *12*, 35856−35872.
(31) Fu, C.-Y.; Chuang, W.-T.; Hsu, S.-h. A Biodegradable Chitosan-Polyurethane Cryogel with Switchable Shape Memory. *ACS Appl. Mater. Interfaces* **2021**, *13*, 9702−9713.
(32) Daksa Ejeta, D.; Wang, C.-F.; Kuo, S.-W.; Chen, J.-K.; Tsai, H.-C.; Hung, W.-S.; Hu, C.-C.; Lai, J.-Y. Preparation of Superhydrophobic and Superoleophilic Cotton-based Material for Extremely High Flux Water-in-oil Emulsion Separation. *Chem. Eng. J.* **2020**, *402*, 126289.
(33) Xu, J.; Xu, M.; Zhao, Y.; Wang, S.; Tao, M.; Wang, Y. Spatial-Temporal Distribution and Evolutionary Characteristics of Water Environment Sudden Pollution Incidents in China from 2006 to 2018. *Sci. Total Environ.* **2021**, *801*, 149677.
(34) Manohara, H. M.; Nayak, S. S.; Franklin, G.; Nataraj, S. K.; Mondal, D. Progress in Marine Derived Renewable Functional Materials and Biochar for Sustainable Water Purification. *Green Chem.* **2021**, *23*, 8305−8331.
(35) Zhang, T.; Li, Z.; Lü, Y.; Liu, Y.; Yang, D.; Li, Q.; Qiu, F. Recent Progress and Future Prospects of Oil-Absorbing Materials. *Chin. J. Chem. Eng.* **2019**, *27*, 1282−1295.
(36) Hu, Y.; Liu, X.; Zou, J.; Gu, T.; Chai, W.; Li, H. Graphite/Isobutylene-isoprene Rubber Highly Porous Cryogels as New Sorbents for Oil Spills and Organic Liquids. *ACS Appl. Mater. Interfaces* **2013**, *5*, 7737−7742.
(37) Chen, X.; Sui, W.; Ren, D.; Ding, Y.; Zhu, X.; Chen, Z. Synthesis of Hydrophobic Polymeric Cryogels with Supermacroporous Structure. *Macromol. Mater. Eng.* **2016**, *301*, 659−664.
(38) Haleem, A.; Wang, J. Y.; Li, H. J.; Hu, C. S.; Li, X. C.; He, W. D. Macroporous Oil-Sorbents with a High Absorption Capacity and High-Temperature Tolerance Prepared Through Cryo-Polymerization. *Polymers* **2019**, *11*, 1620.
(39) Haleem, A.; Li, H.-J.; Li, P.-Y.; Hu, C.-S.; Li, X.-C.; Wang, J.-Y.; Chen, S.-Q.; He, W.-D. Rapid UV-Radiation Synthesis of Polyacrylate Cryogel Oil-Sorbents with Adaptable Structure and Performance. *Environ. Res.* **2020**, *187*, 109488.
(40) Guo, F.; Wang, Y.; Chen, M.; Wang, C.; Kuang, S.; Pan, Q.; Ren, D.; Chen, Z. Lotus-Root like Supermacroporous Cryogels with Superphilicity for Rapid Separation of Oil-Inwater Emulsions. *ACS Appl. Polym. Mater.* **2019**, *1*, 2273−2281.
(41) Zhu, Z.; Jiang, L.; Liu, J.; He, S.; Shao, W. Sustainable, Highly Efficient and Superhydrophobic Fluorinated Silica Functionalized Chitosan Aerogel for Gravity-Driven Oil/Water Separation. *Gels* **2021**, *7*, 66.
(42) Su, C.; Yang, H.; Zhao, H.; Liu, Y.; Chen, R. Recyclable and Biodegradable Superhydrophobic and Superoleophilic Chitosan Sponge for The Effective Removal of Oily Pollutants from Water. *Chem. Eng. J.* **2017**, *330*, 423−432.
(43) Bidgoli, H.; Khodadadi, A. A.; Mortazavi, Y. A Hydrophobic/Oleophilic Chitosan-Based Sorbent: Toward an Effective Oil Spill Remediation Technology. *J. Environ. Chem. Eng.* **2019**, *7*, 103340.
(44) Chen, C.; Weng, D.; Mahmood, A.; Chen, S.; Wang, J. Separation Mechanism and Construction of Surfaces with Special Wettability for Oil/Water Separation. *ACS Appl. Mater. Interfaces* **2019**, *11*, 11006−11027.
(45) Zhang, W.; Liu, N.; Cao, Y.; Lin, X.; Liu, Y.; Feng, L. Superwetting Porous Materials for Wastewater Treatment: from Immiscible Oil/Water Mixture to Emulsion Separation. *Adv. Mater. Interfaces* **2017**, *4*, 1600029.
(46) Xu, C.; Zhan, W.; Tang, X.; Mo, F.; Fu, L.; Lin, B. Self-Healing Chitosan/Vanillin Hydrogels Based on Schiff-Base Bond/Hydrogen Bond Hybrid Linkages. *Polym. Test.* **2018**, *66*, 155−163.
(47) Wang, Y.; Di, J.; Wang, L.; Li, X.; Wang, N.; Wang, B.; Tian, Y.; Jiang, L.; Yu, J. Infused-Liquid-Switchable Porous Nanofibrous Membranes for Multiphase Liquid Separation. *Nat. Commun.* **2017**, *8*, 575.
(48) Chaudhary, J. P.; Vadodariya, N.; Nataraj, S. K.; Meena, R. Chitosan-Based Aerogel Membrane for Robust Oil-in-Water Emulsion Separation. *ACS Appl. Mater. Interfaces* **2015**, *7*, 24957−24962.
(49) Xu, L.; Chen, Y.; Liu, N.; Zhang, W.; Yang, Y.; Cao, Y.; Lin, X.; Wei, Y.; Feng, L. Breathing Demulsification: A Three-Dimensional (3D) Free-Standing Superhydrophilic Sponge. *ACS Appl. Mater. Interfaces* **2015**, *7*, 22264−22271.
(50) Shi, J.; Zhang, H.; Wang, Q.; Duan, Z.; Xu, L.; Guo, F.; Xie, Y.; Chen, Z. Biomimetic Rigid Cryogels with Aligned Micro-sized Tubular Structures Prepared by Conventional Redox-induced Cryopolymerization in a Freezer. *Chem. Eng. J.* **2022**, *427*, 131903.
(51) Zhao, M.; Tao, Y.; Wang, J.; He, Y. Facile Preparation of Superhydrophobic Porous Wood for Continuous Oil Water Separation. *J. Water Proc. Eng.* **2020**, *36*, 101279.
(52) Nozawa, A.; Ohnuma, T.; Sekine, T. Re-Examination of the Microanalysis of Non-Ionic Surfactants That Contain Polyoxyethylene Chains by the Method Involving Solvent Extraction of the Thiocyanatocobaltate(II) Complex. *Analyst* **1976**, *101*, 543−548.


https://doi.org/10.1021/acsomega.1c06178
*ACS Omega* 2022, 7, 5937−5945